



Global Biogeochemical Cycles

RESEARCH ARTICLE

10.1002/2013GB004728

Key Points:

- Global warming reduces seawater viscosity, thus accelerating particle sinking
- Faster sinking enhances the biological pump and oceanic carbon uptake
- This “viscosity effect” is a previously overlooked climate feedback mechanism

Correspondence to:

J. Taucher,
jtaucher@geomar.de

Citation:

Taucher, J., L. T. Bach, U. Riebesell, and A. Oschlies (2014), The viscosity effect on marine particle flux: A climate relevant feedback mechanism, *Global Biogeochem. Cycles*, 28, doi:10.1002/2013GB004728.

Received 9 SEP 2013

Accepted 5 MAR 2014

Accepted article online 13 MAR 2014

The viscosity effect on marine particle flux: A climate relevant feedback mechanism

J. Taucher^{1,2}, L. T. Bach^{1,2}, U. Riebesell¹, and A. Oschlies¹
¹GEOMAR Helmholtz Centre for Ocean Research Kiel, Kiel, Germany, ²equal contribution

Abstract Oceanic uptake and long-term storage of atmospheric carbon dioxide (CO₂) are strongly driven by the marine “biological pump,” i.e., sinking of biotically fixed inorganic carbon and nutrients from the surface into the deep ocean (Sarmiento and Bender, 1994; Volk and Hoffert, 1985). Sinking velocity of marine particles depends on seawater viscosity, which is strongly controlled by temperature (Sharqawy et al., 2010). Consequently, marine particle flux is accelerated as ocean temperatures increase under global warming (Bach et al., 2012). Here we show that this previously overlooked “viscosity effect” could have profound impacts on marine biogeochemical cycling and carbon uptake over the next centuries to millennia. In our global warming simulation, the viscosity effect accelerates particle sinking by up to 25%, thereby effectively reducing the portion of organic matter that is respired in the surface ocean. Accordingly, the biological carbon pump’s efficiency increases, enhancing the sequestration of atmospheric CO₂ into the ocean. This effect becomes particularly important on longer time scales when warming reaches the ocean interior. At the end of our simulation (4000 A.D.), oceanic carbon uptake is 17% higher, atmospheric CO₂ concentration is 180 ppm lower, and the increase in global average surface temperature is 8% weaker when considering the viscosity effect. Consequently, the viscosity effect could act as a long-term negative feedback mechanism in the global climate system.

1. Introduction

In the surface ocean, inorganic carbon and nutrients are converted photosynthetically into organic matter by phytoplankton. As the carbon passes through the food web, most of it is converted back to CO₂ via respiration and released to the atmosphere. However, a small fraction of this organic matter escapes remineralization and is exported from the euphotic zone to deeper waters as sinking particles (“export production”). The biological pump plays a major role in the global carbon cycle [Sarmiento and Bender, 1994; Volk and Hoffert, 1985], and it has been estimated that atmospheric CO₂ concentrations would be more than twice as high without this mechanism [Maier-Reimer et al., 1996].

Various studies have shown that climate change might have pronounced impacts on marine primary production, export of organic matter, and consequently on the efficiency of the biological pump and associated oceanic uptake of atmospheric CO₂ [Bopp et al., 2001; Boyd and Doney, 2002; Passow and Carlson, 2012; Riebesell et al., 2009]. No study to date however has addressed the potential effects of changing seawater viscosity on the sinking of organic matter, although a relationship between seawater viscosity and sinking velocity of marine particles has long been recognized [Smyda, 1970]. Generally, gravitationally accelerated particles move faster at lower viscosities. As rising temperatures reduce seawater viscosity, the sinking velocity of particles will accelerate (Figures 1a and 1c). Recent projections of climate change estimate an increase in global surface temperatures of 1.1 to 6.4°C until 2100 A.D. and more in the following centuries [Intergovernmental Panel on Climate Change, 2007]. Empirical evidence shows that the associated changes in seawater viscosity may accelerate sinking velocities of natural marine particles such as zooplankton fecal pellets or marine aggregates by ~5%/°C warming, with yet unknown consequences for carbon sequestration in the oceans [Bach et al., 2012; Honjo and Roman, 1978]. Here we use an earth system model (University of Victoria Earth System Climate Model (UVic ESCM)) to specifically investigate the potential global effect of temperature-driven changes in seawater viscosity on the sinking and export of organic matter and discuss associated implications on marine biogeochemical cycling and a potential climate feedback.

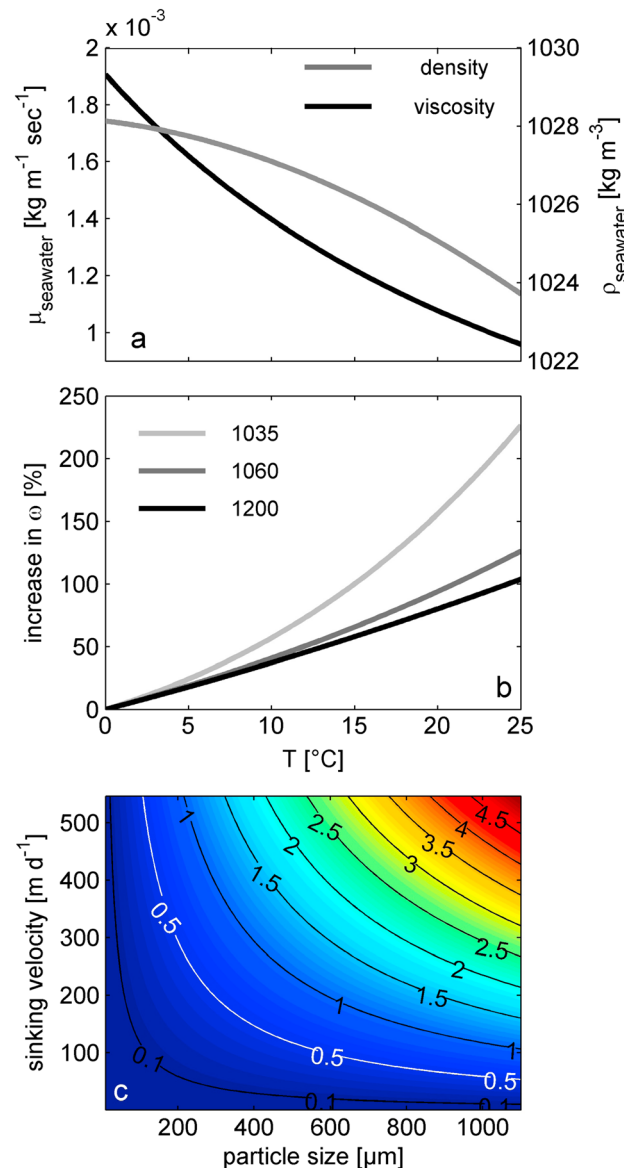


Figure 1. Physical basics for the viscosity effect. (a) Temperature dependence of viscosity (black) and density (gray) of seawater. (b) Relative increase of sinking velocity (ω) with increasing temperature. Different lines denote different particle densities: 1035 kg m⁻³ (light gray), 1060 kg m⁻³ (gray), and 1200 kg m⁻³ (black). (c) Reynolds number in relation to particle size and sinking velocity. White line denotes the threshold beyond which particle sinking might begin to transition from a laminar flow into a turbulent regime.

[Berelson, 2002; Clegg and Whitfield, 1990; Martin et al., 1987]. This in turn is usually attributed to an increase in mean size and density of particles due to preferential remineralization of smaller and less dense particles.

To investigate the impact of changing viscosity on marine particle flux, the NPZD ecosystem model was applied in two different configurations. The CONTROL model corresponds to a version applied in several previous studies [Schmittner et al., 2008; Taucher and Oeschies, 2011], whereas the VISCOSITY model contains a modified parameterization for sinking of organic matter, where sinking velocity is dependent on seawater viscosity as described below.

2. Methods

We applied an earth system model of intermediate complexity (UVic ESCM) including a marine ecosystem model that simulates the cycling of nutrients (N), phytoplankton (P), zooplankton (Z), and detritus (D). Biomass produced photosynthetically by phytoplankton is grazed upon by zooplankton and ultimately channeled into the pool of detrital organic matter. In turn, the loss of detritus occurs as (1) particle sinking, thereby representing the biological pump, and as (2) heterotrophic remineralization, which attenuates the vertical particle flux. The aim of this study is to investigate the impact of changing seawater viscosity on sinking speed of particles and associated flux of organic matter to the deep ocean. The sinking velocity of spherical particles can generally be calculated with Stokes' law:

$$\omega = \frac{2}{9} \times g \times r^2 \times \frac{\rho_{\text{particle}} - \rho_{\text{seawater}}}{\mu_{\text{seawater}}} \quad (1)$$

where ω is the sinking velocity of a particle, g is the Earth's gravitational acceleration (9.81 m s⁻¹), r is the radius of the particle, and ρ_{particle} and ρ_{seawater} are the density of the particle and the seawater, respectively. Accordingly, particle-sinking velocity increases with decreasing viscosity and increasing excess density of the particle compared to seawater density. Data from sediment traps suggest that the observed vertical pattern of particulate organic carbon (POC) flux, decreasing exponentially from the surface to the deep ocean, is associated with an increase in sinking velocity with depth

In the CONTROL model, particle sinking velocity is calculated as

$$\omega_D = \omega_{D0} + m_\omega z \quad (2)$$

Sinking speed (ω_D) at the sea surface is set to 6.0 m d^{-1} (ω_{D0}) and increases linearly with depth (z), i.e., to $\sim 45 \text{ m d}^{-1}$ at 1000 m and $\sim 90 \text{ m d}^{-1}$ at 2000 m by applying the factor m_ω (set to 0.04 d^{-1}). While changes in particle size and density are not explicitly represented in the applied model, this common parameterization of sinking velocity as a function of depth is consistent with estimates of POC flux and can be considered a reasonable approximation to observed conditions [Kriest and Oeschlies, 2008]. However, the sensitivity to environmental change may not be reflected correctly in equation (2). Accordingly, we test the impact of temperature-related changes in seawater viscosity on the vertical particle flux in the VISCOSITY model experiment. The dynamic viscosity of seawater (μ_{seawater}) is a function of pressure, salinity, and temperature, among which temperature is by far the most important factor in a marine system [Bett and Cappi, 1965; Sharqawy et al., 2010]. The μ_{seawater} almost doubles from 25 to 0°C (Figure 1a), thereby showing considerable spatial and temporal variability. Based on Stokes' law (equation (1)), the temperature sensitivity of viscosity and the influence of excess density are included in the calculation of sinking velocity in the VISCOSITY model (ω_μ), which is given as

$$\omega_\mu = \alpha(z) \times \frac{\mu(0^\circ\text{C})}{\mu(T)} \times \frac{\rho_{\text{part}} - \rho_{\text{seawater}(T)}}{\rho_{\text{part}} - \rho_{\text{seawater}(0^\circ\text{C})}} \quad (3)$$

This term consists of three parts: a term that describes the temperature-driven viscosity effect on sinking velocity, a term that describes the influence of assumed excess particle density on the strength of the viscosity effect, and the dynamic coefficient $\alpha(z)$. The latter is necessary to obtain similar global mean vertical profiles of sinking velocity for preindustrial conditions as in the CONTROL model (i.e., a linear increase of sinking speed with depth), thereby facilitating the comparability of the different model setups. Since both the term for the viscosity effect and the term for the density effect decrease exponentially in the upper few hundred meters of the water column (as temperature decreases and approaches the reference temperature of 0°C , equation (3)), the coefficient α is a nonlinear function of depth:

$$\alpha = \alpha(z) = 0.04078z + \frac{1212}{(254.3 + z)} - 1.493 \quad (4)$$

with z is measured in meters. The equation for $\alpha(z)$ was obtained by inserting globally averaged vertical profiles of viscosity and density for preindustrial conditions into equation (3) and fitting the coefficient α in a way to achieve the same vertical profile of preindustrial sinking velocity as in the CONTROL model (equation (2)). Note that the main term in the equation for $\alpha(z)$ is a linear function (similar to equation (2)), while the additional nonlinear term was introduced to better reproduce the sinking velocity profile of the CONTROL model in the upper few hundred meters of the water column.

For particle density, we assume an average of 1060 kg m^{-3} (equation (3)) in the VISCOSITY model, which is based on estimates from literature [Bach et al., 2012; Logan and Hunt, 1987]. However, since the viscosity-related increase in sinking velocity is modified by the density difference between particles and seawater (Figure 1b and equation (3)), we also created model setups to test the effect of assumed particle densities of 1035 and 1200 kg m^{-3} , i.e., one value near the density of seawater and another value for higher density particles (e.g., diatoms or calcifying organisms), as well as a model setup without an effect of particle density on sinking velocity at all. While the absolute values were slightly different between the model setups, the overall patterns and dynamics were very similar to the VISCOSITY model setup with 1060 kg m^{-3} . Results from these additional experiments are therefore not shown in this study.

Furthermore, the validity of sinking velocity according to Stokes' law depends on the Reynolds number, which is in turn a function of the size and shape of the particle, as well as the sinking velocity. For reasons of simplicity, we did not implement a full particle size spectrum model, as this is not necessary for the effects of viscosity investigated here. Assuming average particle size to be smaller than $1000 \mu\text{m}$ and sinking

Table 1. Differences Between the Model Simulation Without (CONTROL) and Including the Viscosity Effect (VISCOSITY) in Export Production (at 130 m Depth), Sequestration Flux (at 1000 m Depth), and Other Climate Relevant Variables

	CONTROL	VISCOSITY
Export production, 2000 A.D. (GtC yr^{-1})	6.56	6.37
Export production, 4000 A.D. (GtC yr^{-1})	6.85	6.55
Export production, relative change between 2000 and 4000 A.D. (%)	+4.4	+2.8
Sequestration flux, 2000 A.D. (GtC yr^{-1})	0.74	0.70
Sequestration flux, 4000 A.D. (GtC yr^{-1})	0.47	0.63
Sequestration flux, relative change between 2000 and 4000 AD (%)	−36.5	−10.0
Atmospheric CO_2 , 4000 A.D. (ppm)	1500	1320
Net cumulative oceanic carbon uptake between 1780 and 4000 A.D. (GtC)	2061	2415
Global average increase in surface air temperature between 2000 and 4000 A.D. ($^{\circ}\text{C}$)	7.7	7.1

velocities not exceeding 150 m d^{-1} , which is reasonable for the largest portion of marine particles that contribute to particle mass flux [Clegg and Whitfield, 1990; Jackson *et al.*, 1997; McDonnell and Buesseler, 2010; Stemmann *et al.*, 2004], Reynolds numbers remain largely below a critical value in the ocean depth range important for the biological pump effects investigated in this study (Figure 1c). It should be kept in mind however that the deviations from Stokes' law might potentially occur when large particles sink fast enough for turbulence to develop.

3. Results and Discussion

3.1. Present Day

As can be expected from the physical relationship between temperature and viscosity, there are some regional differences in sinking velocity in the contemporary ocean between the CONTROL model with climate-independent constant sinking velocity, and the VISCOSITY model, in which the rate of particle sinking varies spatially and temporally as a function of local water temperature and viscosity (see section 2). Sinking velocity in the VISCOSITY model is faster in the tropical surface ocean and slower in the Arctic compared to the CONTROL model with a constant particle sinking rate. However, the impact of these differences on the large-scale distribution of biogeochemical tracers in the ocean is relatively small, and the present-day conditions of nutrient and oxygen fields are simulated almost equally well in both models. Compared to the data from the World Ocean Atlas [Garcia *et al.*, 2010], the global average root-mean-square (RMS) error for simulated phosphate in 2000 is $0.152 \text{ mmol m}^{-3}$ and $0.156 \text{ mmol m}^{-3}$ in the CONTROL and VISCOSITY model, respectively. This RMS error is at the lower end of errors found for biogeochemical tracers in previous modeling studies [Doney *et al.*, 2009; Kriest *et al.*, 2010]. The biological rates in 2000 A.D. are also in the same range in both models. Global net primary productivity (NPP) reaches 59.4 GtC yr^{-1} in the CONTROL run and 53.6 GtC yr^{-1} in the VISCOSITY run. Export production (at 130 m depth) amounts to 6.56 and 6.37 GtC yr^{-1} in the respective models (Table 1). The slight differences between these numbers originate from spatial differences between the models. Since viscosity is an inverse function of temperature, sinking velocity and thus export production follow the spatial pattern of water temperature and are lower at high latitudes and higher in the tropics in the VISCOSITY compared to the CONTROL simulation.

3.2. Long-Term Simulation

Following the Special Report on Emissions Scenarios A2 until 2100 A.D., and a subsequent linear decrease of emissions to zero in 2300 A.D., simulated global sea surface temperatures increase from a global average of $\sim 18^{\circ}\text{C}$ to $\sim 24^{\circ}\text{C}$ around 2400 A.D. and stay almost constant thereafter. However, the warming signal continues to penetrate into the ocean interior over the course of the simulation (Figure 2a), thereby increasing sinking velocity in the upper ($<1000 \text{ m}$) ocean by more than 20% in the VISCOSITY model (Figure 2b). At the end of the model simulations (4000 A.D.), export production amounts to 6.85 and 6.55 GtC yr^{-1} in the CONTROL and VISCOSITY model, respectively, and is thus even slightly higher than under present-day conditions (Table 1). NPP increases even stronger (+53% and +29% in the CONTROL and in the VISCOSITY model) between 2000 and 4000 A.D. (Table 1). This increase is mainly attributable to the direct effect of warming on metabolic rates. As both phytoplankton growth

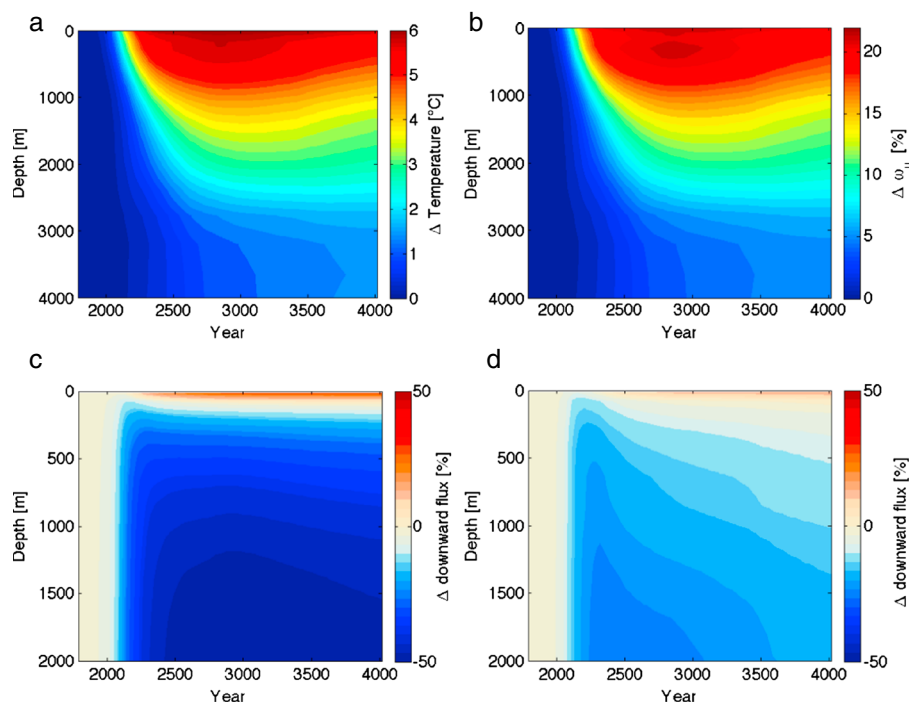


Figure 2. (a) Vertical profile of change relative to preindustrial conditions in the global mean ocean temperature in the VISCOSITY model and (b) associated global mean change in sinking velocity (%) in the VISCOSITY model. Change relative to preindustrial conditions (%) of the global mean vertical particle flux in the (c) CONTROL and (d) VISCOSITY model.

and remineralization processes are positively affected by increasing temperatures, the turnover of organic matter in the surface ocean is accelerated; i.e., NPP is fueled by rapidly regenerated nutrients. This also explains the divergent response of NPP and export production to climate change [Taucher and Oeschlies, 2011]. The different magnitude of change in NPP between the two model setups results from differences in nutrient availability. The viscosity effect leads to faster particle sinking under global warming, thereby stripping nutrients out of the euphotic zone more efficiently and transporting them to the ocean interior. Consequently, fewer nutrients are available to fuel NPP in the surface ocean in the VISCOSITY model (Figures 3a and 3b).

3.3. Viscosity Effect on the Biological Pump

While the response of export production to climate change is very similar in both models, the sequestration flux [Lampitt *et al.*, 2008], i.e., the carbon flux to the ocean interior (here defined as >1000 m depth) that removes atmospheric CO_2 on the time scale of centuries, reveals substantial differences between the two models. In 2000 A.D., this “sequestration flux” amounts to 0.74 and 0.70 GtCyr^{-1} in the CONTROL and VISCOSITY run, respectively. In response to climate change, the carbon flux to the deep ocean decreases and remains below the preindustrial level in both models, an effect which is mainly driven by the accelerating effect of increasing temperatures on the remineralization of organic matter (Figures 2c and 2d). At the end of the simulation (4000), the sequestration flux is 0.47 and 0.63 GtCyr^{-1} in the CONTROL and VISCOSITY run, respectively, with the decrease being much lower in the VISCOSITY run (−10%) than in the CONTROL run (−36%) (Table 1). Thus, the weakening of the biological pump due to climate change is strongly reduced when the viscosity effect on particle sinking velocity is considered.

The reason for this discrepancy between export production and sequestration flux is the different attenuation of the sinking flux of organic matter in the two models (Figures 2c and 2d). In the CONTROL model, where sinking velocity remains constant under ocean warming but remineralization rates

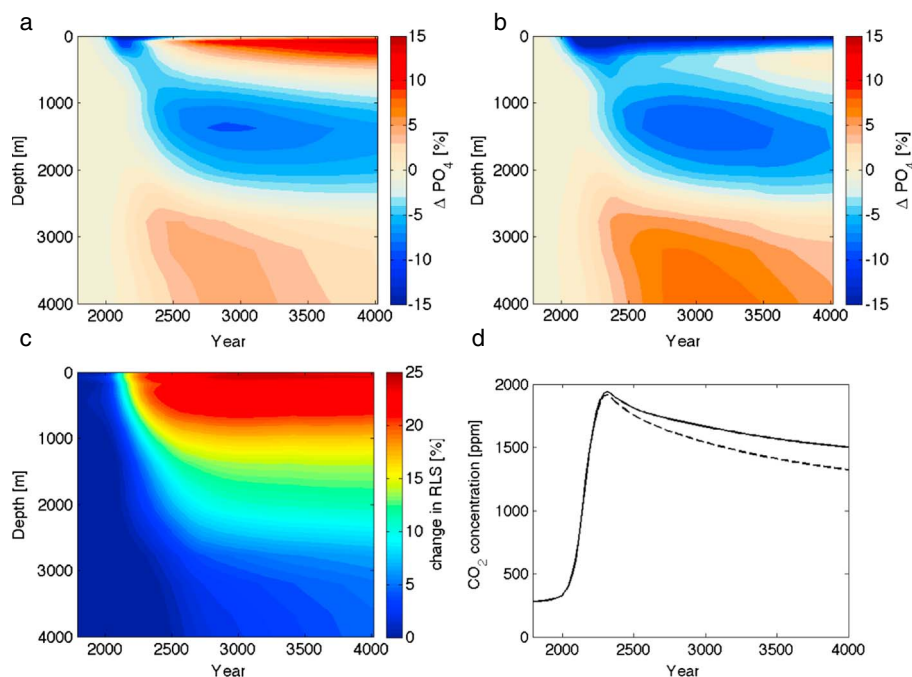


Figure 3. Vertical profile of change relative to preindustrial conditions (%) in the global mean phosphate in the (a) CONTROL and (b) VISCOSITY model. (c) Vertical profile of the relative difference in remineralization length scale between the VISCOSITY and CONTROL model (%). Increasingly, red areas denote for the relatively longer RLS in the VISCOSITY compared to the CONTROL run. (d) Atmospheric CO_2 concentrations in the CONTROL (solid) and VISCOSITY simulation (dashed).

increase with temperature, sinking particles are decomposed to a larger extent within the upper few hundred meters of the ocean (i.e., the mesopelagic zone), thereby decreasing the portion of organic matter that sinks to the deeper ocean (Figure 4). By contrast, increasing sinking velocities in the VISCOSITY model counteract accelerated heterotrophic decomposition in a warming ocean. This results in a more effective removal of organic matter from the surface ocean compared to the CONTROL run. Therefore, the efficiency of the biological pump in the future ocean is positively influenced by the viscosity effect, as a larger portion of organic matter escapes turnover through remineralization in the upper few hundred meters of the water column and reaches the deep ocean in this model setup (Figure 4). In other words, the warming-induced increase in sinking velocity in the VISCOSITY model increases the remineralization length scale (RLS); i.e., the distance it takes until a certain amount of organic matter is respired (Figure 3c).

These results show that the carbon export to the deep ocean (and thereby effective long-term removal of carbon) is more effective when the influence of temperature-driven viscosity changes on particle sinking is taken into account. The net cumulative carbon uptake of the ocean over the course of the simulation (1780 to 4000) amounts to 2415 GtC in the VISCOSITY model, compared to 2061 GtC in the CONTROL model, and is thus 17% higher when considering the viscosity effect. This is also confirmed by the lower concentrations of atmospheric CO_2 at the end of the simulation, which amount to 1320 ppm in the VISCOSITY run compared to 1500 ppm in the CONTROL model (Figure 3d and Table 1). Correspondingly, the global mean surface temperatures in 4000 A.D. are 0.6°C lower, and the global warming is reduced by 8% with the viscosity effect being considered (Table 1). These findings confirm that slight changes in remineralization depth can have notable effects on oceanic carbon uptake and consequently atmospheric CO_2 concentrations [Kwon *et al.*, 2009].

3.4. Time Scale of the Viscosity Effect

While warming of the surface follows climate change-driven atmospheric temperature increases on short time scales, the penetration of the warming signal to deeper layers is much slower, as it largely depends

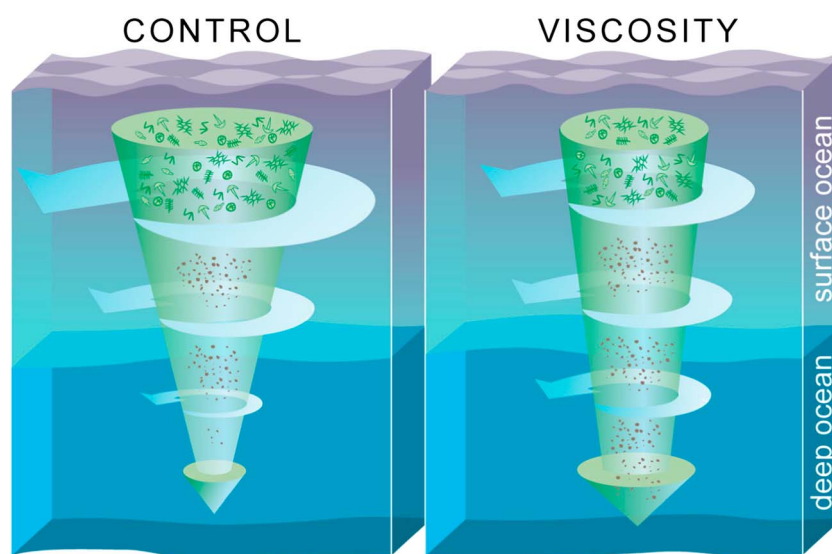


Figure 4. Schematic diagram on the influence of the viscosity effect on particulate organic matter export in a warmer future ocean as simulated without (CONTROL) and including the viscosity effect on particle sinking velocity (VISCOSITY). Under CONTROL conditions, ocean warming does not reduce viscosity and therefore has no effect on sinking velocity. Compared to the VISCOSITY model, sinking particles remain longer above sequestration depth so that a larger fraction can be remineralized (illustrated by the green “particle flux arrow” with greater attenuation and the larger circular blue “respiration arrows”) in the surface ocean. When the viscosity effect is implemented, particle sinking is accelerated and a larger fraction of organic matter escapes remineralization above sequestration depth. Thus, the remineralization length scale (the distance a particle sinks until a certain amount of organic matter is respired) is longer in the VISCOSITY model, which is indicated by a weaker attenuation of the green particle flux arrow and the—over the water column—more homogeneously distributed blue respiration arrows. Furthermore, the higher efficiency of the biological pump (i.e., sinking of organic matter to the deep ocean) in the VISCOSITY setup leads to a stronger decrease in surface ocean nutrient concentrations and therefore lower primary production and plankton standing stocks. This is indicated by the lower number of green phytoplankton particles in the surface box. Consequently, the warming of the surface ocean results in a faster cycle of primary production and remineralization in the CONTROL model. Accelerated particle sinking velocities in the VISCOSITY model counteract this effect and enhance the efficiency of the biological carbon pump.

on physical transport via mixing and the meridional overturning circulation. Since the viscosity effect is directly coupled to changing seawater temperatures, it affects the global system on similar time scales as the warming signal is distributed in the ocean interior, i.e., centuries to millennia (Figures 2a–2d). An instantaneous impact of the viscosity effect on elemental cycling in the 21st century is largely restricted to water masses situated above the winter mixed layer, i.e., depths < 1000 m. This limits the immediate feedback of the viscosity effect on the atmospheric CO₂ concentration, as the organic matter sequestration flux to water masses not in contact with the atmosphere is only slightly affected during this initial period (Figure 3d). A significant influence of the viscosity effect on the atmospheric carbon dioxide concentration arises therefore most prominently on longer time scales in our model runs. However, it has been suggested recently that the global warming signal is transferred into the mesopelagic zone much faster than previously estimated, with 30% of the warming having occurred below 700 m over the last decade [Balmeda *et al.*, 2013]. Such an accelerated penetration of warming to the ocean interior is not yet resolved by current earth system models and would allow for a much more rapid evolution of the viscosity effect than presented in our simulations.

4. Conclusion

Our findings demonstrate for the first time the potential global impact of temperature-driven changes in seawater viscosity on marine particle flux and consecutive changes in biogeochemical element cycling and carbon uptake of the oceans. The viscosity effect in response to ocean warming positively influences the efficiency of the biological pump and results in a larger remineralization length scale. As a larger portion of organic matter reaches the deep ocean, this ultimately increases the long-term

sequestration of carbon in the ocean interior. Since the viscosity effect could potentially act as a previously overlooked negative climate feedback, we suggest that this effect should be considered in future studies investigating long-term effects of climate change.

Acknowledgments

This study was supported by the Deutsche Forschungsgemeinschaft and the Federal Ministry of Education and Research (BMBF) in the framework of the BIOACID project. We also thank Rita Erven for her assistance with graphical illustration. Furthermore, we thank two anonymous reviewers and the editorial office for their constructive comments on the manuscript.

References

- Bach, L. T., U. Riebesell, S. Sett, S. Febiri, P. Rzepka, and K. G. Schulz (2012), An approach for particle sinking velocity measurements in the 3–400 μm size range and considerations on the effect of temperature on sinking rates, *Mar. Biol.*, 159(8), 1853–1864, doi:10.1007/s00227-012-1945-2.
- Balmaseda, M. A., K. E. Trenberth, and E. Källén (2013), Distinctive climate signals in reanalysis of global ocean heat content, *Geophys. Res. Lett.*, 40, 1754–1759, doi:10.1002/grl.50382.
- Berelson, W. M. (2002), Particle settling rates increase with depth in the ocean, *Deep Sea Res. Part II*, 49(1–3), 237–251, doi:10.1016/S0967-0645(01)00102-3.
- Bett, K. E., and J. B. Cappi (1965), Effect of pressure on the viscosity of water, *Nature*, 207(4997), 620–621.
- Bopp, L., P. Monfray, O. Aumont, J. L. Dufresne, H. Le Treut, G. Madec, L. Terray, and J. C. Orr (2001), Potential impact of climate change on marine export production, *Global Biogeochem. Cycles*, 15(1), 81–99, doi:10.1029/1999GB001256.
- Boyd, P. W., and S. C. Doney (2002), Modelling regional responses by marine pelagic ecosystems to global climate change, *Geophys. Res. Lett.*, 29(16), 1806, doi:10.1029/2001GL014130.
- Clegg, S. L., and M. Whitfield (1990), A generalized model for the scavenging of trace metals in the open ocean. I. Particle cycling, *Deep Sea Res. Part A*, 37(5), 809–832, doi:10.1016/0198-0149(90)90008-j.
- Doney, S. C., I. Lima, J. K. Moore, K. Lindsay, M. J. Behrenfeld, T. K. Westberry, N. Mahowald, D. M. Glover, and T. Takahashi (2009), Skill metrics for confronting global upper ocean ecosystem-biogeochemistry models against field and remote sensing data, *J. Mar. Syst.*, 76(1–2), 95–112, doi:10.1016/j.jmarsys.2008.05.015.
- Garcia, H. E., R. A. Locarnini, T. P. Boyer, J. I. Antonov, M. M. Zweng, O. K. Baranova, and D. R. Johnson (2010), *World Ocean Atlas 2009, Volume 4: Nutrients (phosphate, nitrate, silicate)*, pp. 398, U.S. Government Printing Office, Washington, D. C.
- Honjo, S., and M. R. Roman (1978), Marine copepod fecal pellets - Production, preservation and sedimentation, *J. Mar. Res.*, 36(1), 45–57.
- IPCC (2007), *Climate Change 2007: The Physical Science Basis, Contribution of Working Group I to the Fourth Assessment Report of the Intergovernmental Panel on Climate Change*, pp. 996, Cambridge Univ. Press, Cambridge, U. K., and New York.
- Jackson, G. A., R. Maffione, D. K. Costello, A. L. Alldredge, B. E. Logan, and H. G. Dam (1997), Particle size spectra between 1 μm and 1 cm at Monterey Bay determined using multiple instruments, *Deep Sea Res. Part I*, 44(11), 1739–1767, doi:10.1016/s0967-0637(97)00029-0.
- Kriest, I., and A. Oschlies (2008), On the treatment of particulate organic matter sinking in large-scale models of marine biogeochemical cycles, *Biogeosciences*, 5(1), 55–72, doi:10.5194/bg-5-55-2008.
- Kriest, I., S. Khaliwala, and A. Oschlies (2010), Towards an assessment of simple global marine biogeochemical models of different complexity, *Prog. Oceanogr.*, 86(3–4), 337–360, doi:10.1016/j.pcean.2010.05.002.
- Kwon, E. Y., F. Primeau, and J. L. Sarmiento (2009), The impact of remineralization depth on the air-sea carbon balance, *Nat. Geosci.*, 2(9), 630–635, doi:10.1038/ngeo612.
- Lampitt, R. S., et al. (2008), Ocean fertilization: A potential means of geoengineering?, *Philos. Trans. R. Soc. London, Ser. A*, 366(1882), 3919–3945, doi:10.1098/rsta.2008.0139.
- Logan, B. E., and J. R. Hunt (1987), Advantages to microbes of growth in permeable aggregates in marine systems, *Limnol. Oceanogr.*, 32(5), 1034–1048.
- Maier-Reimer, E., U. Mikolajewicz, and A. Winguth (1996), Future ocean uptake of CO_2 : Interaction between ocean circulation and biology, *Clim. Dyn.*, 12(10), 711–722, doi:10.1007/s003820050138.
- Martin, J. H., G. A. Knauer, D. M. Karl, and W. W. Broenkow (1987), VERTEX - Carbon cycling in the Northeast Pacific, *Deep Sea Res. Part A*, 34(2), 267–285, doi:10.1016/0198-0149(87)90086-0.
- McDonnell, A. M. P., and K. O. Buesseler (2010), Variability in the average sinking velocity of marine particles, *Limnol. Oceanogr.*, 55(5), 2085–2096, doi:10.4319/lo.2010.55.5.2085.
- Passow, U., and C. A. Carlson (2012), The biological pump in a high CO_2 world, *Mar. Ecol. Prog. Ser.*, 470, 249–271, doi:10.3354/meps09985.
- Riebesell, U., A. Kortzinger, and A. Oschlies (2009), Sensitivities of marine carbon fluxes to ocean change, *Proc. Natl. Acad. Sci. U.S.A.*, 106(49), 20,602–20,609, doi:10.1073/pnas.0813291106.
- Sarmiento, J. L., and M. Bender (1994), Carbon biogeochemistry and climate-change, *Photosynth. Res.*, 39(3), 209–234, doi:10.1007/bf00014585.
- Schmittner, A., A. Oschlies, H. D. Matthews, and E. D. Galbraith (2008), Future changes in climate, ocean circulation, ecosystems, and biogeochemical cycling simulated for a business-as-usual CO_2 emission scenario until year 4000 AD, *Global Biogeochem. Cycles*, 22, GB1013, doi:10.1029/2007GB002953.
- Sharqawy, M. H., J. H. Lienhard, and S. M. Zubair (2010), The thermophysical properties of seawater: A review of existing correlations and data, *Desalin. Water Treat.*, 16, 354–380, doi:10.5004/dwt.2010.1079.
- Smayda, T. (1970), The suspension and sinking of phytoplankton in the sea, in *Oceanography and Marine Biology: An Annual Review*, vol. 8, pp. 353–414, Taylor & Francis, London, U. K.
- Stemmann, L., G. A. Jackson, and G. Gorsky (2004), A vertical model of particle size distributions and fluxes in the midwater column that includes biological and physical processes - Part II: Application to a three year survey in the NW Mediterranean Sea, *Deep Sea Res. Part I*, 51(7), 885–908, doi:10.1016/j.dsr.2004.03.002.
- Taucher, J., and A. Oschlies (2011), Can we predict the direction of marine primary production change under global warming?, *Geophys. Res. Lett.*, 38, L02603, doi:10.1029/2010GL045934.
- Volk, T., and M. I. Hoffert (1985), Ocean carbon pumps: Analysis of relative strengths and efficiencies in ocean-driven atmospheric CO_2 changes, in *The Carbon Cycle and Atmospheric CO_2 : Natural Variations Archean to Present*, *Geophys. Monogr. Ser.*, vol. 32, edited by E. T. Sundquist and W. S. Broecker, pp. 99–110, AGU, Washington, D. C.